

Efficient removal of toxic methylene blue (MB) dye from aqueous solution using a metal-organic framework (MOF) MIL-101(Fe): isotherms, kinetics, and thermodynamic studies

Abdelazeem S. Eltaweil^{a,*}, Eman M. Abd El-Monaem^a, Ahmed M. Omer^{b,*}, Randa E. Khalifa^a, Mona M. Abd El-Latif^c, Gehan M. El-Subruiti^a

^aChemistry Department, Faculty of Science, Alexandria University, Alexandria, Egypt, emails: abdelazeem_s_eltaweil@hotmail.com (A.S. Eltaweil), emanabdelmonaem5925@yahoo.com (E.M. Abd El-Monaem), randaghonim@yahoo.com (R.E. Khalifa), profgehan@yahoo.com (G.M. El-Subruiti)

^bPolymer Materials Research Department, Advanced Technology and New Materials Research Institute, SRTA-City, New Borg El-Arab City, P.O. Box: 21934, Alexandria, Egypt, email: Ahmedomer_81@yahoo.com (A.M. Omer)

^cFabrication Technology Department, Advanced Technology and New Materials Research Institute, SRTA-City, New Borg El-Arab City, P.O. Box: 21934, Alexandria, Egypt, email: amona1911@yahoo.com (M.M. Abd El-Latif)

Received 30 May 2019; Accepted 22 January 2020

ABSTRACT

MIL-101(Fe) iron-benzene dicarboxylate based metal-organic framework (MOF) was synthesized via a solvothermal method for adsorptive removal of cationic methylene blue (MB) dye from aqueous solution. The prepared MIL-101(Fe) was characterized by X-ray diffraction, Fourier transform infrared spectroscopy, scanning electron microscopy, transmission electron microscopy, thermal gravimetric analyzer, X-ray photoelectron spectroscopy, and Brunauer–Emmett–Teller analysis tools. Various parameters affecting the removal efficiency were deliberated such as pH medium, contact time, solution temperature, MOF dosage, and initial MB dye concentrations. Results showed that MIL-101(Fe) has a maximum adsorption capacity of 58.82 mg/g at pH 9. Moreover, data obtained from isotherm studies were more fitted to the Langmuir isotherm model ($R^2 = 0.997$), while the adsorption kinetics followed the pseudo-second-order model. The thermodynamic studies proved that the adsorption process of MB dye onto MIL-101(Fe) was spontaneous and endothermic. Besides, MIL-101(Fe) showed higher adsorption ability towards cationic MB dye compared to the anionic methyl orange dye. Finally, the MIL-101(Fe) adsorbent showed excellent reusability for removing MB dye with efficiency exceeded 70% after ten consecutive cycles. Therefore, the as-prepared MIL-101(Fe) could be applied as a reusable adsorbent for removing cationic dyes from their aqueous solutions.

Keywords: Metal-organic framework; MIL-101(Fe); MB dye removal; Kinetics; Reusability

1. Introduction

The color decoration is an essential part of many industries including papers, printing, refineries, cosmetics, and food processing [1]. Effluents discharged from these

industries contain large quantities of dye residues, which greatly causes harmful effects on human health owing to their chemical stability and non-biodegradability [2–4]. Moreover, the photosynthesis process of aquatic plants may be inhibited by the presence of these dyes as they reduce the

* Corresponding authors.

entering light [5]. Methylene blue (MB) is one of the most common cationic dye members, that extensively applied in several industries such as textile dyeing, leather, plastics, human and veterinary pharmacopoeia [6,7]. Although MB dye has several harmful impacts such as short durations of difficulty breathing, nausea, vomiting and gastritis troubles [8]. Therefore, various physical, chemical and biological techniques have been applied for the treatment of dyes-contaminated effluents such as coagulation, oxidation, catalysis, photocatalysis, adsorption, membrane filtration, and biosorption [9–17].

Adsorption method is a powerful technique for removing dye-contaminants owing to its unique advantages such as low-cost, simplicity, production of minimal secondary pollutants and easy regeneration [12]. Various adsorbents have been used for the treatment of dye-contaminated effluents including natural occurring adsorbents such as activated carbon [18], clays [19], zeolites [20], siliceous materials [21], agricultural waste materials [22] and polymeric adsorbents [12,23].

Metal-organic frameworks (MOFs) are a group of porous hybrid materials, consist of metal ions and multifunctional organic linkers and exhibit highly ordered structures with high crystallinity. Recently, MOFs have attracted much attention owing to their excellent features such as higher surface area, porosity, and higher thermal stability [24]. Therefore, MOFs materials have been widely used in various applications including gas storage and separation, imaging, catalysis, and drug delivery filed [25–27]. Extensive developments have been made for MOFs based-adsorbents for removing heavy metals [28,29], toxic dyes [30,31] and pharmaceutical residual [32–34]. Till now, several types of MOFs materials such as MOF-235 [35], Uio-66 [36], Fe(BzC) [37], Cu-BDC [38], TMU-16 [39] and MIL-101(Al) [40] have been applied for adsorption of organic dyes. However, there are no studies on the adsorption of cationic MB dye using MIL-101(Fe). Herein, we aimed to prepare MIL-101(Fe) using ferric chloride hexahydrate and terephthalic acid as an adsorbent for MB dye. The prepared adsorbent was characterized using Fourier transform infrared spectroscopy (FTIR), thermal gravimetric analyzer (TGA), scanning electron microscopy (SEM), transmission electron microscopy (TEM), X-ray photoelectron spectroscopy (XPS) and Brunauer–Emmett–Teller (BET) characterization tools. The influence of different adsorption conditions on the adsorptive removal of cationic MB dye was studied, while the ability of MIL-101(Fe) to adsorb anionic methyl orange (MO) dye was also investigated. Moreover, adsorption isotherm, thermodynamics, and kinetic studies were also explored. Besides, the reusability of the developed adsorbent was examined using several adsorption–desorption cycles.

2. Experimental

2.1. Materials

Ferric chloride hexahydrate ($\text{FeCl}_3 \cdot 6\text{H}_2\text{O}$, 99.0%), *N,N*-dimethylformamide (DMF, 99.5%) were supplied by Sigma-Aldrich (USA), terephthalic acid (H_2BDC , 98.0%) and ethanol ($\text{C}_2\text{H}_5\text{OH}$) were obtained from Merck (Germany). MB trihydrate was supplied from BDH Company (UK) and its characteristics are listed in Table S1. MO dye was purchased

from Aladdin Industrial Corporation (Shanghai, China), all chemicals and solvents were used as received without further purifications.

2.2. Synthesis of MIL-101(Fe)

MIL-101(Fe) was prepared according to the previously reported method [41] with a slight modification. In a typical experiment, $\text{FeCl}_3 \cdot 6\text{H}_2\text{O}$ (0.196 g) and H_2BDC (0.325 g) were dissolved in 30 mL of DMF solution under vigorous stirring conditions for 10 min at room temperature. Thereafter, the mixture was transferred into a 100 mL Teflon autoclave and followed with heating in an oven at 130°C for 24 h. After cooling to room temperature, the solid product was collected by centrifugation and washed repeatedly with DMF and ethanol solutions. Finally, the solid obtained was dried in an air oven at 120°C for 24 h. The schematic diagram describes the preparation method of MIL-101(Fe) and digital images before and after MB dye adsorption is represented in Fig. 1.

2.3. Characterization

The chemical structure of the as-prepared MIL-101(Fe) was investigated by Fourier transform infrared spectroscopy (FTIR-Shimadzu-8400S, Japan), X-ray diffraction was analyzed using X-ray diffractometer (XRD-BRUKER D8 Advance Cu target, Germany). Moreover, the thermal behavior was examined by thermal gravimetric analyzer (TGA-Shimadzu-50, Japan). The surface morphology of the prepared MIL-101(Fe) was investigated by scanning electron microscope (SEM-JEOL JSM 6360 LA, Japan) along with the transmission electron microscope (TEM-JEOL-2100 plus, Japan). Besides, X-ray photoelectron spectroscopy (XPS-Thermo Fisher Scientific, USA) was used to analyze the surface elements, while N_2 adsorption–desorption isotherm data were observed by using the Brunauer–Emmett–Teller method (BET-Beckman Coulter, SA3100, USA).

2.4. Batch adsorptive removal studies

All adsorption experiments of MB dye were performed in a batch method. Firstly, a stock solution of MB (1,000 mg/L) was prepared and kept in the dark under standard conditions. To investigate the effect of pH on the adsorption process, the pH of MB dye solution was tested over the range 3.0–13.0 and adjusted using 0.1 M of both HCl and NaOH solutions. An accurate dose of adsorbent (0.001–0.03 g) was soaked in 5 mL of MB dye solution with concentrations ranged from 10 to 200 mg/L. To evaluate the effect of adsorption temperature the adsorption, experiments were carried out at different temperatures ranged from 25°C to 55°C. After different time intervals, the used adsorbent was separated using centrifugation at 5,500 rpm for 3 min. After that, the residual concentration of MB dye was determined at $\lambda_{\text{max}} = 664 \text{ nm}$ using a UV-vis spectrophotometer. The removal (%) and the adsorption capacity (q_e) of MB dye were calculated using Eqs. (1) and (2), respectively:

$$\%R = \frac{C_0 - C_t}{C_0} \times 100 \quad (1)$$

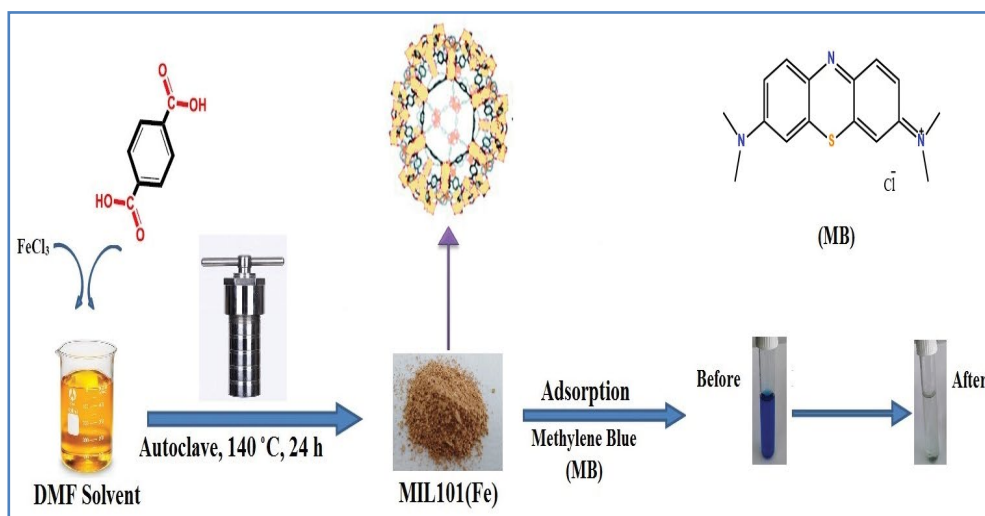


Fig. 1. Schematic diagram for the preparation of MIL-101(Fe) and photos for MB dye before and after adsorption.

$$q_t \text{ (mg/g)} = \frac{(C_0 - C_t) \times V}{m} \quad (2)$$

where q_t (mg/g) is the adsorption capacity of MB dye at time t , C_0 (mg/L) is the initial dye concentration of MB dye, C_t (mg/L) is the concentration of MB dye at time t , m (g) is the mass of the adsorbent and V (L) is the volume of MB dye solution.

Besides, the ability of the prepared MIL-101(Fe) to adsorb MO dye as a model of anionic dyes was also tested. In brief, 0.01 g of MIL-101(Fe) was immersed into 5 mL of MO dye solution with initial concentration 50, 100 and 200 mg/L. The adsorption process was conducted at 25°C, while the adsorption contact time was fixed to 500 min. The adsorbate concentrations after completion of the adsorption process were assayed at 464 nm using UV-vis spectrophotometer.

2.5. Reusability study

To examine the ability of MIL-101(Fe) to reuse for the adsorption of MB dye, the dye adsorbed–MIL-101(Fe) was separated from the adsorption medium after completion of each adsorption cycle. Thereafter, the adsorbent was regenerated using ethanol (98%) and drying in an oven at 100°C for 12 h. The adsorption–desorption process was performed for ten consecutive cycles.

3. Results and discussions

3.1. Instrumental characterization

3.1.1. Fourier transform infrared spectroscopy

FTIR spectra of the organic linker (H_2BDC) and the as-prepared MIL-101(Fe) before and after adsorption of MB dye are shown in Fig. 2a. The spectrum of MIL-101(Fe) shows a peak at 549 cm^{-1} which is ascribed to Fe–O vibration, while the observed peaks at 737 and 862 cm^{-1} are related to the bending vibration of aromatic C–H of the benzene ring, and the peak at 1,120 cm^{-1} is attributed to

C–C bond. Additionally, the symmetric stretching band at 1,390 cm^{-1} and the two asymmetric stretching bands at 1,525 and 1,691 cm^{-1} are corresponding to the present carboxylic group [42]. Besides, the peak at 1,691 cm^{-1} indicates the interaction between the Fe ion and the deprotonated carboxyl group [43]. The asymmetric stretching vibration at 2,980 cm^{-1} is related to aliphatic C–H of DMF solvent [38] and the peak at 3,715 cm^{-1} is attributed to the stretching vibration of the –OH group of water absorbed from the air. By comparing FTIR spectra before and after MB adsorption it was noticed that the intensity of the peaks decreased after adsorption of MB dye onto the MIL-101(Fe), while the peak positions are not shifted.

3.1.2. XRD analysis

XRD patterns (Fig. 2b) show the main diffraction peaks of the as-prepared MIL-101(Fe) at $2\theta = 9.7^\circ, 12.3^\circ, 13.7^\circ, 18.6^\circ, 25^\circ, \text{ and } 28.3^\circ$. The gained results agreed with other previously reported studies [42,44].

3.1.3. Thermal gravimetric analyzer

The thermal behavior of MIL-101(Fe) was studied as presented in Fig. 2c. The results clarified that five weight loss stages were detected with rising temperature up to 800°C, the first weight loss (6.1%) between 28°C and 96°C corresponds to the departure of moisture from the sample (at ambient temperature). The second weight loss (4.3%) between 96°C and 355°C could be related to the departure of the solvent (DMF) and the third weight loss (12.9%) between 355°C and 452°C is due to decomposition of the ligand. The fourth weight loss (35.9%) between 452°C and 541°C is attributed to the decomposition of MIL-101(Fe). The final weight loss (7.5%) between 541°C and 800°C is related to the complete decomposition of the MIL-101(Fe) structure. Based on these results, it could be concluded that MIL-101(Fe) has high thermal stability since the temperature needed to loss its half weight ($T_{50\%}$) was 525°C.

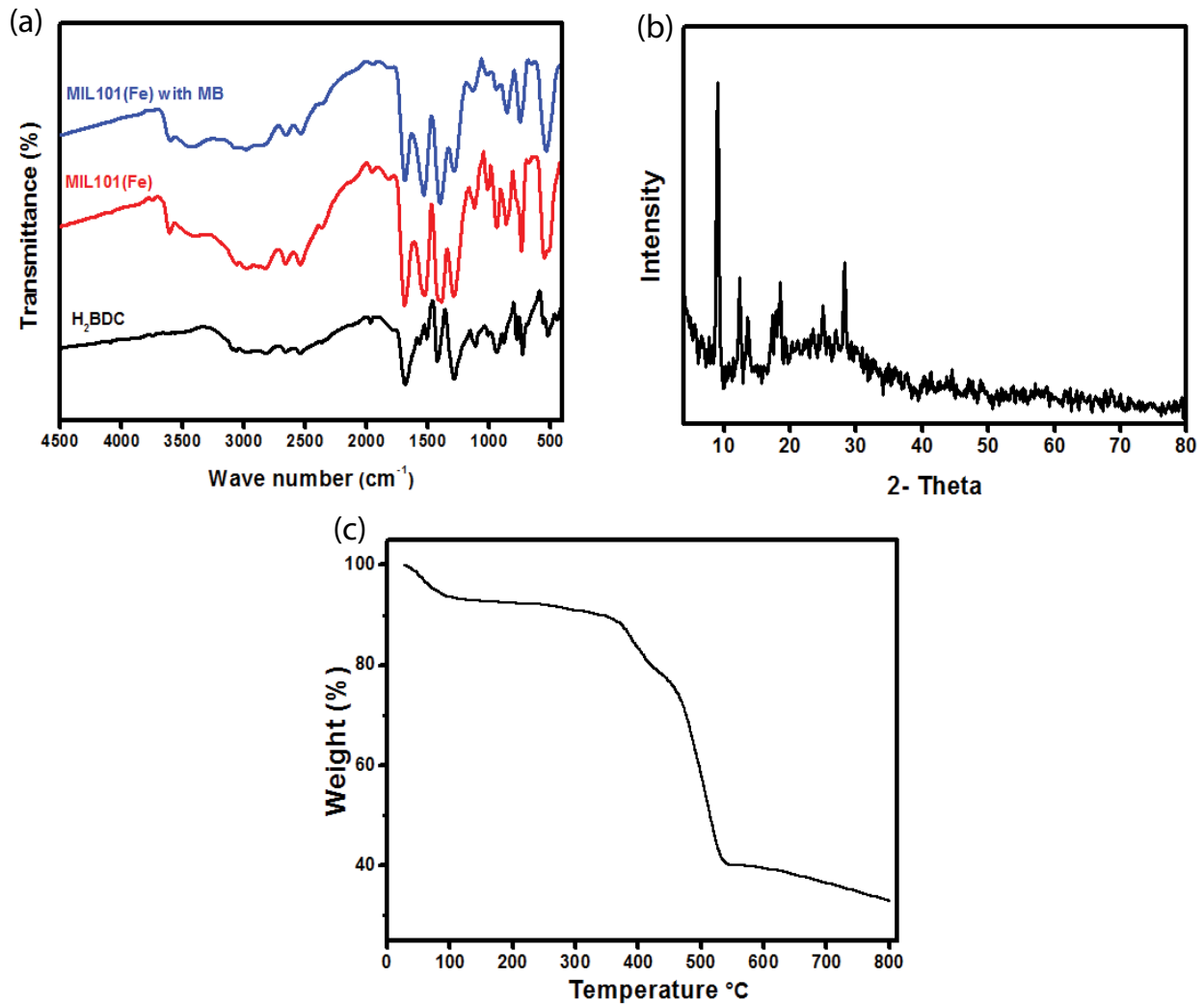


Fig. 2. (a) FTIR, (b) XRD, and (c) TGA of MIL-101(Fe).

3.1.4. Morphological properties

SEM and TEM were used to investigate the morphological properties of the prepared MIL-101(Fe). SEM image (Fig. 3a) clarified that the prepared MIL-101(Fe) adsorbent has almost rod-like particles with an average diameter of ca. 2–3 μm . Moreover, the TEM image (Fig. 3b) showed that MIL-101(Fe) particles have polyhedron shapes with soft edges.

3.1.5. XPS analysis

The XPS characterization provides detailed information on composition and surface binding energy of MIL-101(Fe) as presented in Figs. 4a and b. XPS wide-spectra showed the typical peaks of Fe_{2p}, C1s and O1s in MIL-101(Fe) with additional N1s and S2p peaks upon the adsorption of MB dye. Moreover, the results of XPS indicated that the adsorption of MB on MIL-101(Fe) caused a shift of Fe_{2p} peaks to lower energies (from 711.86 and 724.05 to 711.67 and 722.13 eV), and a shift of O1s peak from 531.83 to 531.48 eV. The occupation of open metal sites in MIL-101(Fe) with water molecules

could be replaced by the stronger Lewis base. Therefore, the interaction between the Lewis base $-\text{N}(\text{CH}_3)_2$ in MB dye and the Lewis acid Fe sites of MIL-101(Fe) could occur. Therefore, MB dye molecules cannot wholly enter through the small pore window of MIL-101(Fe), but it can partially enter the pore of MIL-101(Fe) as the pore window is large enough for its $-\text{N}(\text{CH}_3)_2$ and $-\text{C}_6\text{H}_5$ groups. Moreover, the possibility to establish π - π interaction between the benzene rings in MB and MIL-101(Fe) could be occurred [45].

3.1.6. BET analysis

The N₂ adsorption-desorption isotherm and the pore size distribution for MIL-101(Fe) were investigated and represented in Figs. 4c and d, respectively. The results clarified that MIL-101(Fe) exhibits type II isotherm, which is characteristic for mesoporous material with S_{BET} of 54.711 $\text{m}^2 \text{g}^{-1}$ and pore diameter of 1.66 nm. The low surface area of MIL-101(Fe) indicates that the anhydrous form of MIL-101(Fe) exhibits closed pores with low accessible porosity to N₂ gas.

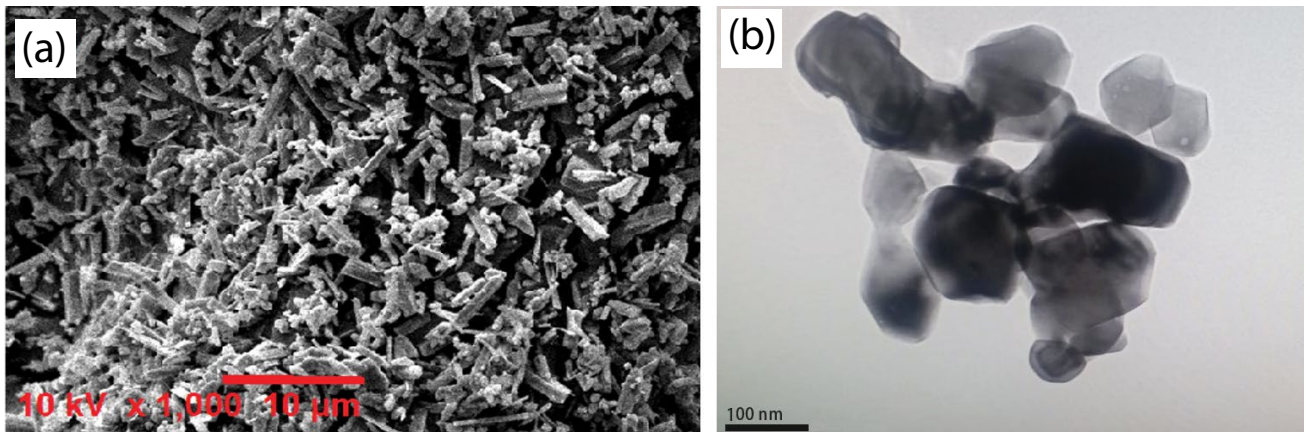


Fig. 3. (a) SEM and (b) TEM images of MIL-101(Fe).

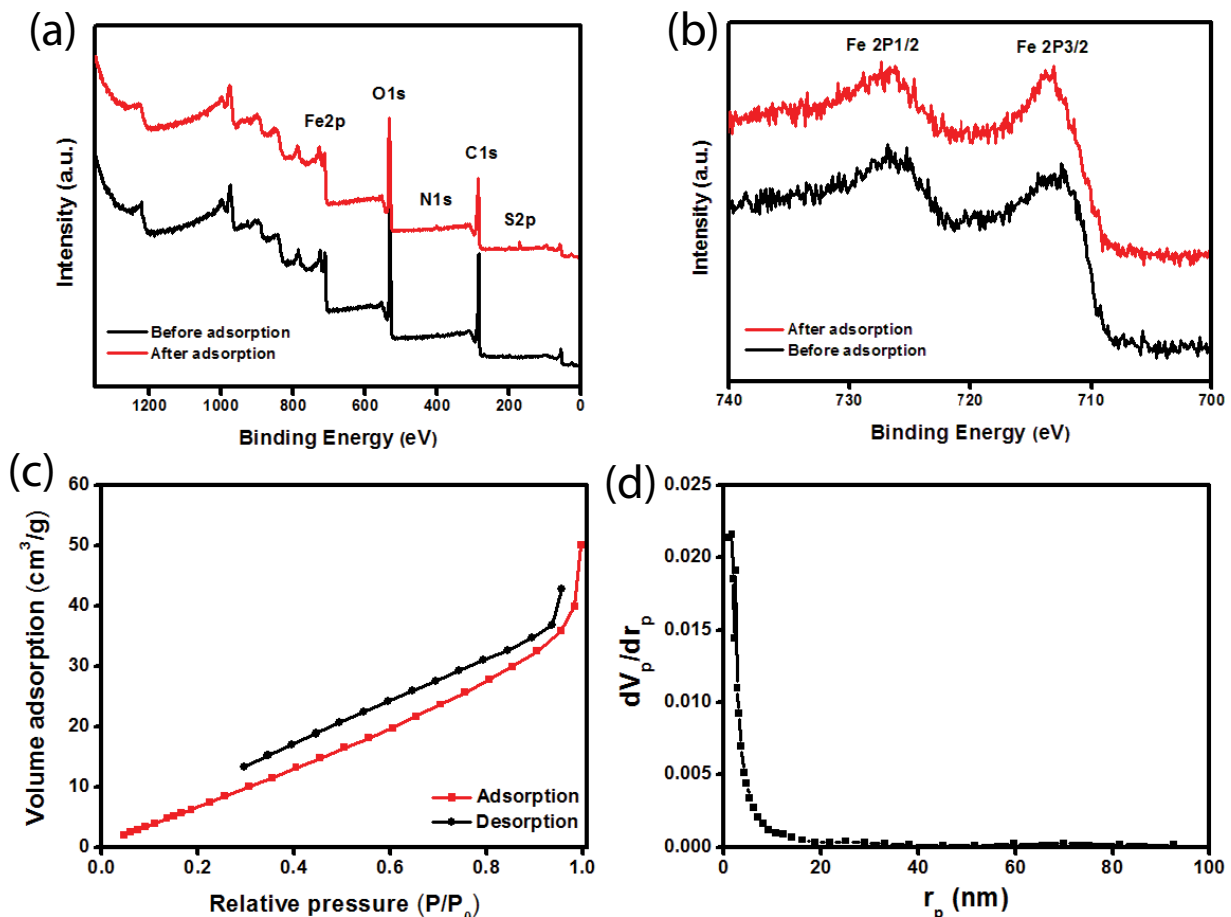


Fig. 4. XPS spectra (a) wide scan and (b) Fe 2p of MIL-101(Fe) before and after adsorption of MB dye.

3.2. Factors affecting MB adsorption

3.2.1. Effect of pH

pH is a significant factor in the adsorption process since it strongly affects the present charges on the adsorbent surface [46]. As shown in Fig. 5a, a maximum removal (%) value was obtained at pH = 9 and recorded 95%.

This behavior is expected for cationic MB dye as reported by Lin et al. [47]. At low pH, H⁺ concentration is high which increases the positive charges on the surface of MIL-101(Fe), and as a result, reduces the adsorption of positively charged MB dye molecules. On the other hand, with increasing pH value, the concentration of H⁺ gradually decreased and the adsorption of MB dye onto MIL-101(Fe) increased till reaches

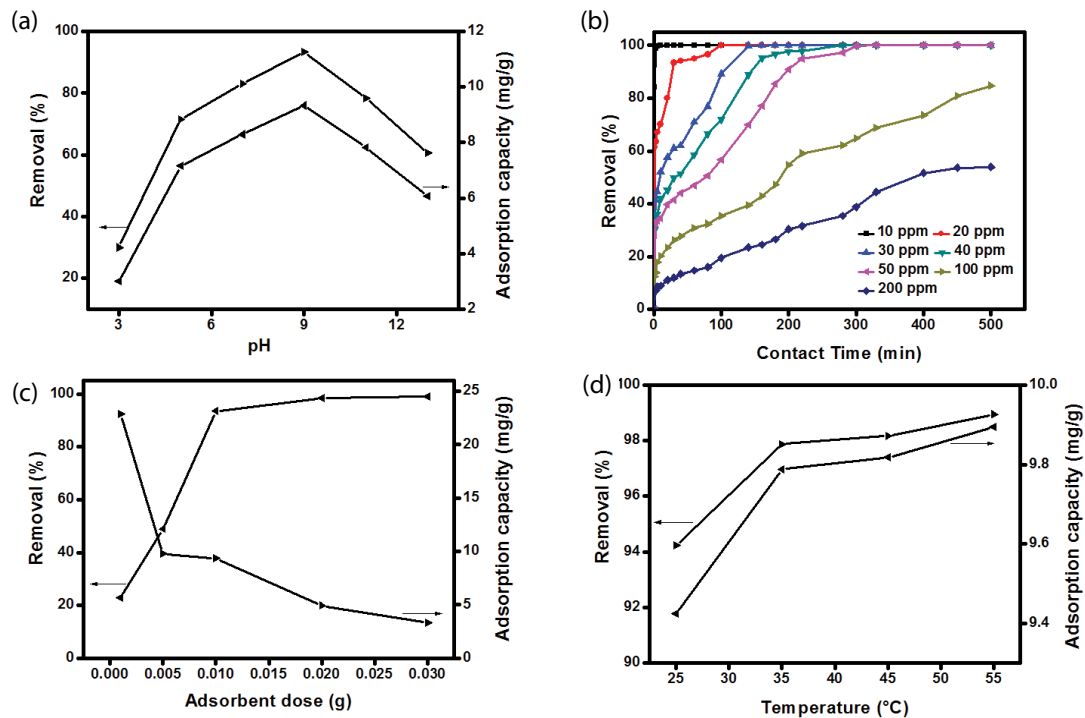


Fig. 5. Effect of (a) pH, (b) initial MB dye concentration, (c) adsorbent dose, and (d) temperature on removal efficiency and adsorption capacity of MB dye.

a maximum value at pH = 9. Thereafter, the adsorption process decreased which could be attributed to the decrease in the solubility of MB dye [48].

3.2.2. Effect of initial MB dye concentration and contact time

It was obvious from Fig. 5b that increasing MB dye concentration up to 200 mg/L decreases the removal (%) values. Besides, the removal rate increases rapidly with increasing the adsorption contact time owing to the abundant vacant adsorption sites on the MIL-101(Fe) surface. After that, the adsorptive removal rate gradually slows down and reaches the equilibrium with a further increase in the contact time. At lower MB dye concentration (i.e. 10 mg/L), MB dye molecules were completely removed after 10 min, while with increasing MB dye concentration up to 50 mg/L, a complete removal was achieved after 300 min from the initial contact time. On the other hand, maximum removal (%) of 84.7% and 54% were reached after 500 min for both 100 and 200 mg/L of MB dye, respectively. These results could be attributed to that, at lower concentrations the available adsorption sites on the MIL-101(Fe) surface are much higher than that needed for MB molecules. Subsequently, a complete MB dye removal occurred, however, the adsorbent surface became saturated gradually with increasing MB dye concentration. Besides, Fig. S1 clarified that values of the adsorption capacity were significantly increased from 5 to 58.82 mg/g with increasing MB dye concentration from 10 to 200 ppm. These results could be explained by increasing the adsorbed amount of MB dye molecules on the surface of MIL-101(Fe) with rising dye concentration up to 200 mg/g.

3.2.3. Effect of adsorbent dosage

The impact of the initial adsorbent dosage is essential for large-scale applications. As shown in Fig. 5c, as the dose of adsorbent, increases the removal (%) rapidly increases until reaches equilibrium at 0.01 g with a maximum removal efficiency of 94%. Increasing the extent of MB removal with increasing the adsorbent dosage could be attributed to increasing the exposed adsorption sites, which make the removal of MB dye molecules more efficient. However, a further increase in the adsorbent dose beyond 0.01 g, has no significant increase in the removal (%), since most MB molecules were removed and the adsorption process reached the equilibrium.

On the other hand, the adsorption capacity gradually decreases with increasing the adsorbent dosage owing to the inverse relationship between the adsorption capacity and the adsorbent dosage as stated previously in Eq. (1). Furthermore, this decline is fundamentally attributable to the aggregation of adsorbent particles as well as the residual unsaturated active sites during the adsorption process with increasing the adsorbent amount [49]. Subsequently, the number of exposed adsorption sites decreases and directly decreases the adsorbed amount of MB dye molecules per unit mass of the MIL-101(Fe). Thus, the adsorption capacity decreases accordingly.

3.2.4. Effect of temperature

Fig. 5d revealed that the removal efficiency and the adsorption capacity values increased with increasing the solution temperature from 25°C to 55°C. However, this

increase in the removal (%) is sharp and noticeable in the range 25°C–35°C, which could be explained by the enhancement in the dispersion of MB dye molecules as well as the significant increment in their diffusion rates toward the surface of adsorbent [50]. Otherwise, there was no significant increase in the removal (%) over the temperature range 35°C–55°C which may be due to the saturation of the majority of the active sites of MIL-101(Fe) with MB molecules. The gained results confirmed that the adsorption process is an endothermic process which has been agreed with the previously reported studies [35].

3.3. Adsorption isotherm models

Adsorption results for the removal of MB dye by MIL-101(Fe) were analyzed using Langmuir, Freundlich and Temkin isotherm models as shown in Fig. 6. Langmuir adsorption model [Eq. (3)] is based on the assumption of monolayer adsorption [51], where the activation energy of each adsorbate on the adsorbent surface is equivalent. Freundlich adsorption isotherm [Eq. (4)] assumes that the adsorption takes place on a multilayer heterogeneous surface with adsorption sites of different adsorption heat [52]. Temkin adsorption isotherm [Eq. (5)] takes into consideration the effect of the interaction between adsorbate and adsorbent. Furthermore, it assumes that the adsorption free energy is changeable along with surface coverage of the

adsorbent [37]. Moreover, a dimensionless separation factor R_L [Eq. (6)] was used to indicate the adsorption favorability. Also, the value B [Eq. (7)] is a constant related to the heat of adsorption (J/mol).

$$\frac{C_e}{q_e} = \frac{1}{bq_m} + \frac{C_e}{q_m} \tag{3}$$

$$\log q_e = \log K_F + \frac{1}{n} \log C_e \tag{4}$$

$$q_e = B \ln A + B \ln C_e \tag{5}$$

$$R_L = \frac{1}{1 + bC_0} \tag{6}$$

$$B = \frac{RT}{b} \tag{7}$$

where q_e (mg/g) represents the adsorption capacity at equilibrium, C_e (mg/L) is the concentration of un-adsorbed adsorbate in solution at equilibrium. Also, A and b are the adsorption constants (L/mg), R is the gas constant (8.314 J/mol k), T is the absolute temperature (K) and q_m (mg/g) refers to the monolayer adsorption capacity.

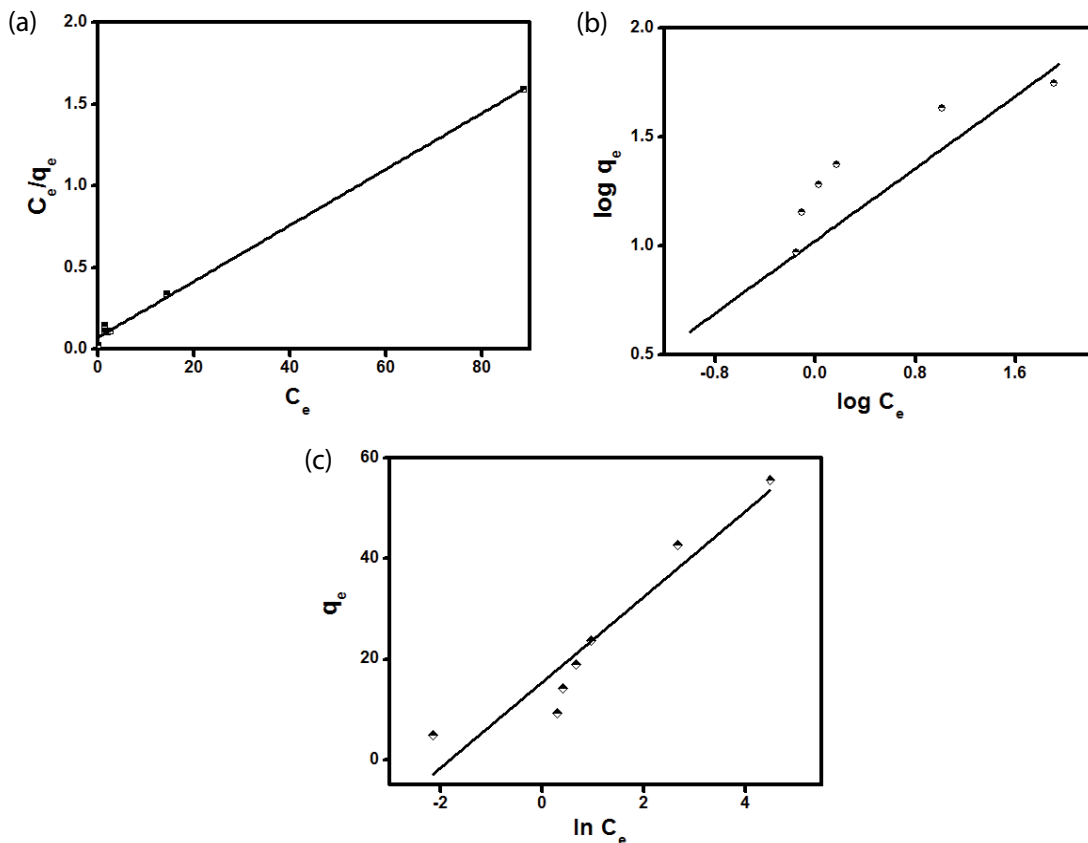


Fig. 6. Isotherm models: (a) Langmuir, (b) Freundlich, and (c) Temkin for the adsorption of MB dye with different initial concentrations (10–200 mg/L) using 0.01 g of MIL-101(Fe), (pH 9) and solution temperature (25°C).

The results obtained from the adsorption isotherm models (Table 1) showed that the adsorption process is more consistent with the Langmuir isotherm model ($R^2 = 0.997$) compared to those of both Freundlich ($R^2 = 0.913$) and Temkin ($R^2 = 0.909$) isotherm models, which reveal that the adsorption of MB dye onto MIL-101(Fe) is a monolayer adsorption.

From the Langmuir isotherm model, q_m was found to be 58.82 mg/g at 298 K. Also, the b value obtained from the Langmuir isotherm was >0 , indicating that the theoretical saturation adsorption capacity surpasses the experimental q_m value [24]. R_L values at all initial concentrations (Table S2) are positive and <1 , which indicates that the adsorption process is favorable. It has been reported that the value of n obtained from Freundlich isotherm gives a clear index for the adsorption behavior. In general, $n < 1$, reveals an unfavorable adsorption, $n = 1$ to 2 express a moderately difficult adsorption and $n = 2$ to 10 demonstrated a favorable adsorption. From Table 3, $n = 2.9$, indicating that the adsorption of MB dye on to MIL-101(Fe) is favorable.

It must be pointed out that the high b value (i.e. $>>80$ kJ/mol) affirms that the adsorption of MB dye on MIL-101(Fe) is a chemical adsorption process. Moreover, the quite high value of b reveals a strong ionic interaction between MB and MIL-101(Fe) [52].

By comparing q_m value of the synthesized MIL-101(Fe) with the values reported in previous studies for removal of MB dye (Table 2), it is evident that MIL-101(Fe) is an efficient adsorbent for removal MB dye.

3.4. Adsorption kinetics

Pseudo-first-order [Eq. (8)] and pseudo-second-order [Eq. (9)] are the two kinetic adsorption models used to fit the experimental data for the adsorption process [53].

$$\ln(q_e - q_t) = \ln q_e - K_1 t \quad (8)$$

$$\frac{t}{q_t} = \frac{1}{K_2 q_e^2} + \frac{1}{q_e} t \quad (9)$$

where q_e and q_t (mg/g) are the adsorption capacity at equilibrium and at time t , K_1 (min^{-1}) and K_2 ($\text{g mg}^{-1} \text{min}^{-1}$) are the rate constants of pseudo-first and pseudo-second-order, respectively. Plots of pseudo-first and pseudo-second-order are shown in Figs. 7a and b. From the kinetic model's parameters (Table 3), it can be concluded that the adsorption process of MB onto MIL-101(Fe) follows the pseudo-second-order model since it has correlation coefficients comparatively higher than those of pseudo-first-order model for the all initial MB dye concentrations. Also, the calculated q_e values from pseudo-second plots are much closer to the

Table 2

Maximum adsorption capacity of MB dye using various adsorbents relative to Langmuir model

Adsorbent	q_m (mg/g)	Ref.
Hydroxyapatite	33.3	[56]
CMC/kC/AMMT beads	12.25	[12]
Rice husk	40.58	[57]
Jute fiber carbon	22.5	[58]
UIO-66	90	[36]
Modified polysaccharide	48	[59]
MIL-101(Fe)	58.82	This study

experimental q_e values than those calculated from pseudo-first plots. Additionally, the rate constants K_2 decreased with increasing the initial MB concentrations revealing that the chemisorption was significant [54].

3.5. Adsorption process mechanism analysis

3.5.1. Intra-particle diffusion model

This model is used to analyze the kinetic results and identify the diffusion mechanism [55]. The linear form of the intra-particle diffusion model is represented by Eq. (10):

$$q_t = K_p t^{0.5} + C \quad (10)$$

where K_p is the intra-particle diffusion rate constant ($\text{mg/g min}^{0.5}$) and C is the intercept.

From the intra-particle diffusion plot (Fig. 8a), it is evident that the adsorption process occurs in three steps. Table 4 shows that the values of C are not equal to zero at all the initial MB dye concentrations which illustrate that the intra-particle diffusion is not the only rate-controlling step. This deviation might be attributable to the difference in the mass transfer rate from the initial to final adsorption stages. Further, the boundary layer thickness is established by the values of the intercept; the more significant the intercept, the higher is the boundary layer consequence. The K_p values increased with increasing the initial dye concentration, indicating that the adsorption of MB dye onto the MIL-101(Fe) is favorable at high concentration and supports improved rate of adsorption.

3.5.2. Boyd model

This model is used to predict the actual rate-determining step in the adsorption process. The Boyd model expression is represented by Eq. (11).

Table 1

Parameters and correlation coefficients of Langmuir, Freundlich and Temkin isotherm models for adsorption of MB dye onto MIL-101(Fe)

Langmuir			Freundlich			Temkin			
b (L/mg)	q_m	R^2	N	K_f (L/mg)	R^2	A (L/mg)	B	b (kJ/mol)	R^2
0.2329	58.82	0.997	2.96	12.25	0.913	6.1	8.507	291.2	0.909

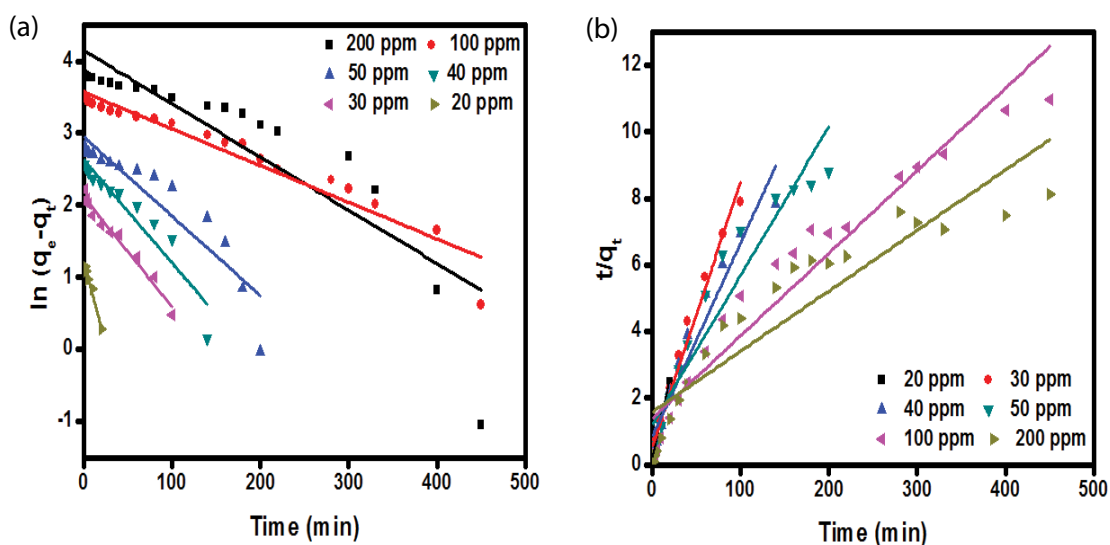


Fig. 7. Kinetic models (a) pseudo-first-order and (b) pseudo-second-order for the adsorption of MB dye with different initial concentrations (10–200 mg/L) using 0.01 g of MIL-101(Fe), (pH 9) and solution temperature (25°C).

Table 3
Kinetic parameters for MB dye adsorption by MIL-101(Fe) at different initial concentrations

Concentration (mg/L)	20	30	40	50	100	200
$q_{e,exp}$ (mg/g)	9.33	14.26	19.04	23.7	42.81	55.7
Pseudo-first-order						
$q_{e,cal}$ (mg/g)	3.39	8.36	13.99	19.16	35.52	63.18
K_1 (min ⁻¹)	0.045	0.015	0.014	0.011	0.005	0.007
R^2	0.985	0.972	0.894	0.858	0.933	0.754
Pseudo-second-order						
$q_{e,cal}$ (mg/g)	8.20	12.66	17.24	22.73	41.67	55.56
K_2 (g mg ⁻¹ min ⁻¹)	0.136	0.0118	0.0041	0.0016	0.0004	0.0002
R^2	0.995	0.982	0.994	0.914	0.938	0.851

$$F = 1 - \frac{6}{\pi^2} \sum_{n=1}^{\infty} \frac{1}{n^2} \exp(-n^2 B_i) \quad (11)$$

where F is the fraction of adsorbate adsorbed at any time ($F = q_t/q_e$).

The B_i (a mathematical function of F) can be calculated from the following Eqs. (12) and (13):

$$B_i = \left(\sqrt{\pi} - \sqrt{\pi - \left(\frac{\pi^2 F}{3} \right)} \right)^2 \quad \text{For } F < 0.85 \quad (12)$$

$$B_i = -0.498 - \ln(1 - F) \quad \text{For } F > 0.85 \quad (13)$$

The Boyd plot (Fig. 8b), indicates that the rate of adsorption was governed by the film-diffusion step whereas the plots for all the initial MB dye concentrations are linear, without passing through the origin.

3.6. Adsorption thermodynamics

Thermodynamic parameters; the change in Gibbs free energy (ΔG°), enthalpy of adsorption (ΔH°) and entropy change (ΔS°) was calculated from the following Eqs. (14) and (15):

$$\Delta G^\circ = -RT \ln K_e \quad (14)$$

$$\ln K_e = \frac{\Delta S^\circ}{R} - \frac{\Delta H^\circ}{RT} \quad (15)$$

From the plot of $\ln K_e$ vs. $1/T$ (Fig. 8c), the entropy and enthalpy values can be estimated from the intercept and slope. The calculated thermodynamic parameters are listed in Table 5. The positive value of ΔH° shows that the adsorption of MB dye over MIL-101(Fe) is endothermic. The positive value of ΔS° specifies the increase in the randomness of the MB dye molecules on the MIL-101(Fe) surface than in the solution. Besides, the negative values of ΔG° at

Table 4
Intra-particle diffusion parameters of adsorption of MB dye

Concentration (mg/L)	K_p , 1–3 (mg g ⁻¹ min ⁻¹)	C	R ²
20	0.432	5.683	0.932
	0.748	4.654	1
	0.135	8.532	0.888
30	0.898	4.554	0.961
	0.892	3.663	0.997
	0.469	8.761	0.936
40	5.315	5.315	0.984
	1.261	1.261	0.98
	15.88	15.88	0.925
50	6.76	6.76	0.988
	7.011	7.011	0.993
	16.98	16.98	0.92
100	8.398	8.398	0.98
	6.545	6.545	0.941
	1.45	1.45	0.989
200	1.277	8.661	0.978
	2.98	9.938	0.946
	0.971	34.23	0.872

all temperatures indicate the feasibility and spontaneously of the adsorption of MB over MIL-101(Fe).

3.7. Adsorption of anionic MO dye

The ability of MIL-101(Fe) to adsorb MO as a model of anionic dyes was investigated using different concentrations of MO dye ranged from 50 to 200 mg/L as presented in Fig. 9a. The results clarified that the maximum adsorption capacity recorded only 11.24 mg/g compared to 58.82 mg/g for cationic MB dye molecules using 200 mg/L of dye concentration and 0.01 g of the adsorbent. These observations could be ascribed to that cationic MB is a basic dye and its Lewis base $-N(CH_3)_2$ groups can easily bind with the active species of the Lewis acid sites of MIL-101(Fe).

Table 5
Parameters of thermodynamics for the adsorption of MB dye onto MIL-101(Fe)

ΔG° (kJ/mol)		ΔH° (kJ/mol)		ΔS° (J/mol K)
298K	308K	318K	328K	
-6.07	-7.75	-9.43	-11.11	43.95
				167.86

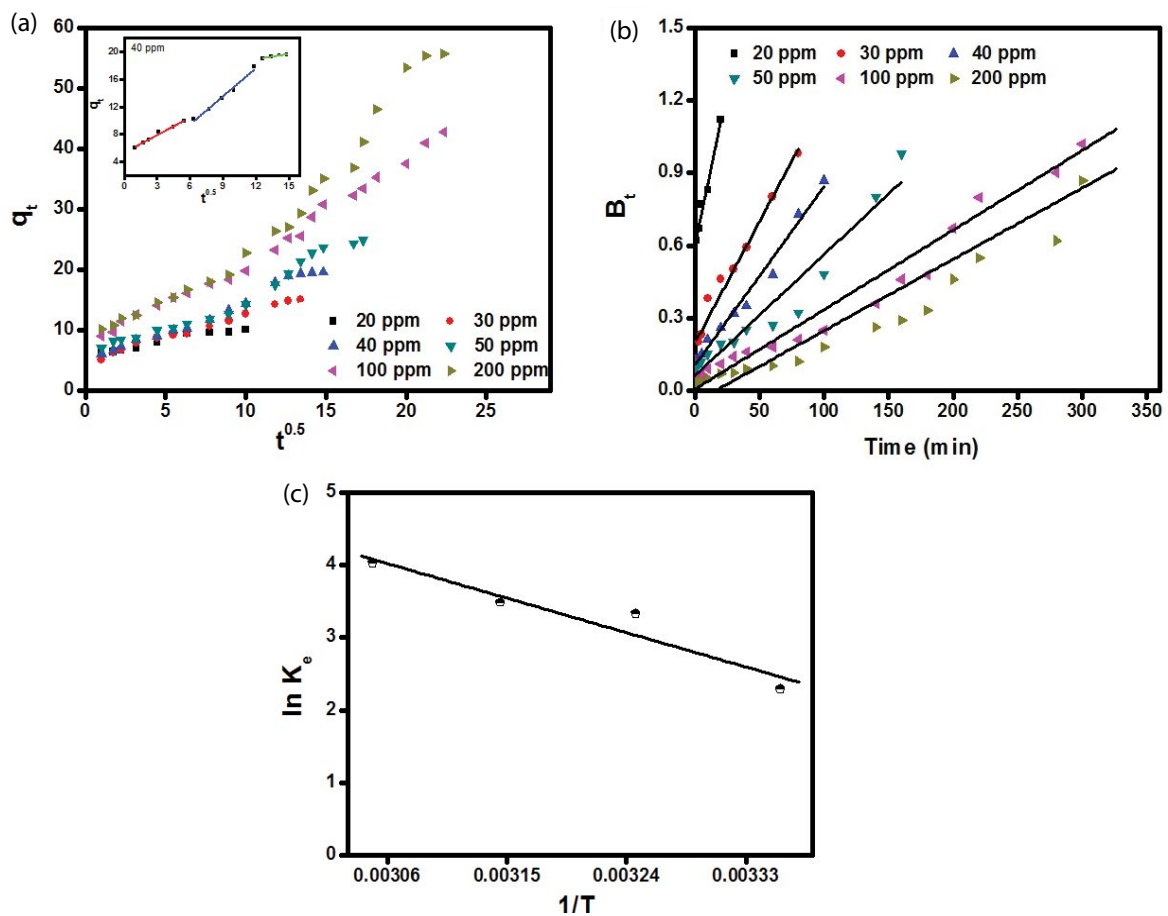


Fig. 8. (a) Intra-particle diffusion model, (b) Boyd model and (c) $\ln K_e$ vs. $1/T$ relationship for adsorption of MB dye onto MIL-101(Fe).

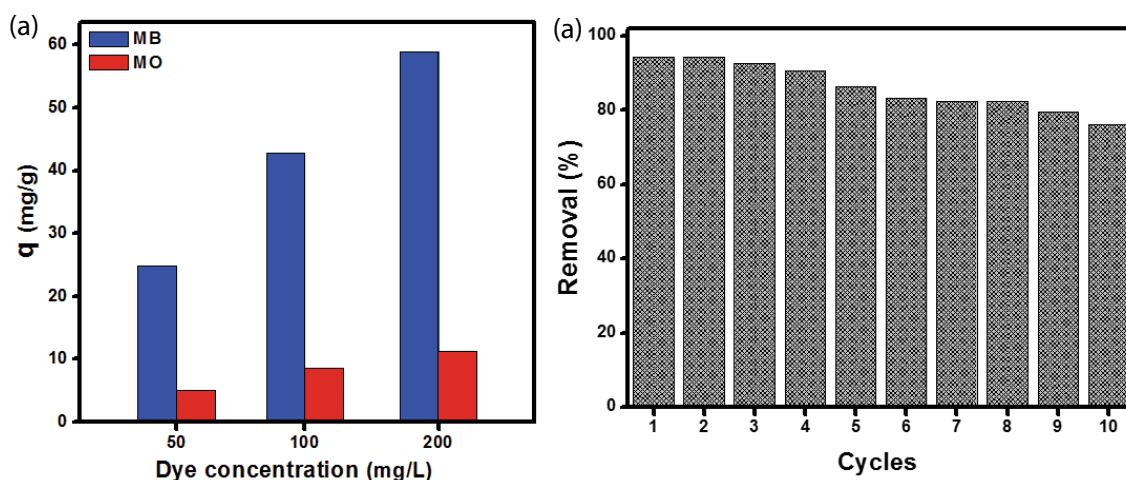


Fig. 9. (a) The adsorption performance of MIL-101(Fe) towards cationic MB and anionic MO dyes, and (b) reusability of MIL-101(Fe) for MB dye removal.

These results proved that the prepared MIL-101(Fe) has the capability to adsorb the cationic dyes much more than the anionic dyes.

3.8. Reusability

The ability of an adsorbent to be regenerated and reused is essential from the economic viewpoint that decreases the production cost. As shown in Fig. 9b, MIL-101(Fe) showed excellent adsorption properties, where the removal (%) of MIL-101(Fe) still higher than 70% after 10 repeated adsorption–desorption cycles.

4. Conclusion

In this study, the MIL-101(Fe) MOF was prepared and characterized using different characterization tools. MIL-101(Fe) was used for adsorption of cationic MB dye from its aqueous solution. Several factors affecting the adsorption process were optimized. The results clarified that the maximum removal (%) was obtained at pH = 9 and 35°C using 10 mg of MIL-101(Fe). The experimental data were fitted with the pseudo-second-order kinetic model and followed the Langmuir isotherm model ($R^2 = 0.997$). The thermodynamic studies indicated that the adsorption process of MB dye over MIL-101(Fe) is spontaneous and endothermic. Furthermore, MIL-101(Fe) showed much higher adsorption ability for the cationic MB dye than anionic MO dye. Besides, the reusability study indicated that MIL-101(Fe) still has an excellent aptitude for the removal of MB dye even after 10 sequential cycles. Therefore, MIL-101(Fe) adsorbent has a great potency for the removal of cationic MB dye from aqueous solutions.

References

- [1] R. Kant, Textile dyeing industry an environmental hazard, *Nat. Sci.*, 4 (2012) 22–26.
- [2] A. Eskhan, F. Banat, M. Selvaraj, M.A. Haija, Enhanced removal of methyl violet 6B cationic dye from aqueous solutions using calcium alginate hydrogel grafted with poly (styrene-co-maleic anhydride), *Polym. Bull.*, (2018) 1–29.
- [3] T.M. Tamer, W.M. Abou-Taleb, G.D. Roston, M.S. Mohyeldin, A.M. Omer, R.E. Khalifa, A.M. Hafez, Formation of Zinc oxide nanoparticles using alginate as a template for purification of wastewater, *Environ. Nanotechnol. Monit. Manage.*, 10 (2018) 112–121.
- [4] M. Elkady, H. Shokry, A. El-Sharkawy, G. El-Subruiti, H. Hamad, New insights into the activity of green supported nanoscale zero-valent iron composites for enhanced acid Blue-25 dye synergistic decolorization from aqueous medium, *J. Mol. Liq.*, 294 (2019) 111628.
- [5] K.A. Adegoke, O.S. Bello, Dye sequestration using agricultural wastes as adsorbents, *Water Resour. Ind.*, 12 (2015) 8–24.
- [6] M.A. El-Latif, A.M. Ibrahim, M. El-Kady, Adsorption equilibrium, kinetics and thermodynamics of methylene blue from aqueous solutions using biopolymer oak sawdust composite, *J. Am. Sci.*, 6 (2010) 267–283.
- [7] F. Raposo, M. De La Rubia, R. Borja, Methylene blue number as useful indicator to evaluate the adsorptive capacity of granular activated carbon in batch mode: influence of adsorbate/adsorbent mass ratio and particle size, *J. Hazard. Mater.*, 165 (2009) 291–299.
- [8] M.A. Haque, M. Shams-Ud-Din, A. Haque, The effect of aqueous extracted wheat bran on the baking quality of biscuit, *Int. J. Food Sci. Technol.*, 37 (2002) 453–462.
- [9] B.H. Hameed, Spent tea leaves: a new non-conventional and low-cost adsorbent for removal of basic dye from aqueous solutions, *J. Hazard. Mater.*, 161 (2009) 753–759.
- [10] M.A.M. Salleh, D.K. Mahmoud, W.A.W.A. Karim, A. Idris, Cationic and anionic dye adsorption by agricultural solid wastes: a comprehensive review, *Desalination*, 280 (2011) 1–13.
- [11] C.R. Holkar, A.J. Jadhav, D.V. Pinjari, N.M. Mahamuni, A.B. Pandit, A critical review on textile wastewater treatments: possible approaches, *J. Environ. Manage.*, 182 (2016) 351–366.
- [12] C. Liu, A. Omer, X.-k. Ouyang, Adsorptive removal of cationic methylene blue dye using carboxymethyl cellulose/k-carrageenan/activated montmorillonite composite beads: isotherm and kinetic studies, *Int. J. Biol. Macromol.*, 106 (2018) 823–833.
- [13] E. El-Sayed, T. Tamer, A. Omer, M. Mohy Eldin, Development of novel chitosan schiff base derivatives for cationic dye removal: methyl orange model, *Desal. Water Treat.*, 57 (2016) 22632–22645.
- [14] S. Sallam, G. El-Subruiti, A. Eltaweil, Facile synthesis of Ag- γ -Fe₂O₃ superior nanocomposite for catalytic reduction of nitroaromatic compounds and catalytic degradation of methyl orange, *Catal. Lett.*, 148 (2018) 3701–3714.

- [15] M.M.A. El-Latif, A.M. Ibrahim, Removal of reactive dye from aqueous solutions by adsorption onto activated carbons prepared from oak sawdust, *Desal. Water Treat.*, 20 (2010) 102–113.
- [16] E. El-Bestawy, A. Mansy, A. Mansee, A. El-Koweidy, Biodegradation of selected chlorinated pesticides contaminating lake Maruit ecosystem, *Pak. J. Biol. Sci.*, 3 (2000) 1673–1680.
- [17] E. El-Bestawy, Efficiency of immobilized cyanobacteria in heavy metals removal from industrial effluents, *Desal. Water Treat.*, 159 (2019) 66–78.
- [18] R. Ahmad, R. Kumar, Adsorptive removal of congo red dye from aqueous solution using bael shell carbon, *Appl. Surf. Sci.*, 257 (2010) 1628–1633.
- [19] T. Shichi, K. Takagi, Clay minerals as photochemical reaction fields, *J. Photochem. Photobiol., C*, 1 (2000) 113–130.
- [20] G. Calzaferri, D. Brühwiler, S. Megelski, M. Pfenniger, M. Pauchard, B. Hennessy, H. Maas, A. Devaux, U. Graf, Playing with dye molecules at the inner and outer surface of zeolite L, *Solid State Sci.*, 2 (2000) 421–447.
- [21] A. Krysztafkiwicz, S. Binkowski, T. Jesionowski, Adsorption of dyes on a silica surface, *Appl. Surf. Sci.*, 199 (2002) 31–39.
- [22] F. Boukhelif, S. Chraïbi, M. Alami, Evaluation of the adsorption kinetics and equilibrium for the potential removal of phenol using a new biosorbent, *J. Environ. Earth Sci.*, 3 (2013) 181–191.
- [23] A. Shebl, A. Omer, T. Tamer, Adsorption of cationic dye using novel O-amine functionalized chitosan Schiff base derivatives: isotherm and kinetic studies, *Desal. Water Treat.*, 130 (2018) 132–141.
- [24] N. Wang, X.-K. Ouyang, L.-Y. Yang, A.M. Omer, Fabrication of a magnetic cellulose nanocrystal/metal-organic framework composite for removal of Pb (II) from water, *ACS Sustainable Chem. Eng.*, 5 (2017) 10447–10458.
- [25] M. Eddaoudi, J. Kim, N. Rosi, D. Vodak, J. Wachter, M. O'keeffe, O.M. Yaghi, Systematic design of pore size and functionality in isorecticular MOFs and their application in methane storage, *Science*, 295 (2002) 469–472.
- [26] F. Ke, Y.-P. Yuan, L.-G. Qiu, Y.-H. Shen, A.-J. Xie, J.-F. Zhu, X.-Y. Tian, L.-D. Zhang, Facile fabrication of magnetic metal-organic framework nanocomposites for potential targeted drug delivery, *J. Mater. Chem.*, 21 (2011) 3843–3848.
- [27] A.H. Chughtai, N. Ahmad, H.A. Younus, A. Laypkov, F. Verpoort, Metal-organic frameworks: versatile heterogeneous catalysts for efficient catalytic organic transformations, *Chem. Soc. Rev.*, 44 (2015) 6804–6849.
- [28] P.A. Kobielska, A.J. Howarth, O.K. Farha, S. Nayak, Metal-organic frameworks for heavy metal removal from water, *Coord. Chem. Rev.*, 358 (2018) 92–107.
- [29] H.T.M. Thanh, T.T.T. Phuong, P.T. Le Hang, T.T.T. Toan, T.N. Tuyen, T.X. Mau, D.Q. Khieu, Comparative study of Pb (II) adsorption onto MIL-101 and Fe-MIL-101 from aqueous solutions, *J. Environ. Chem. Eng.*, 6 (2018) 4093–4102.
- [30] J. Qiu, Y. Feng, X. Zhang, M. Jia, J. Yao, Acid-promoted synthesis of UiO-66 for highly selective adsorption of anionic dyes: adsorption performance and mechanisms, *J. Colloid Interface Sci.*, 499 (2017) 151–158.
- [31] M.R. Azhar, H.R. Abid, H. Sun, V. Periasamy, M.O. Tadé, S. Wang, One-pot synthesis of binary metal organic frameworks (HKUST-1 and UiO-66) for enhanced adsorptive removal of water contaminants, *J. Colloid Interface Sci.*, 490 (2017) 685–694.
- [32] A.R. Abbasi, M. Karimi, M.Y. Masoomi, Effect of construction method and surface area for nano metal-organic framework HKUST-1 upon adsorption and removal of phenazopyridine hydrochloride, *Colloids Surf., A*, 520 (2017) 193–200.
- [33] Z. Hasan, N.A. Khan, S.H. Jhung, Adsorptive removal of diclofenac sodium from water with Zr-based metal-organic frameworks, *Chem. Eng. J.*, 284 (2016) 1406–1413.
- [34] S. Dhaka, R. Kumar, A. Deep, M.B. Kurade, S.-W. Ji, B.-H. Jeon, Metal-organic frameworks (MOFs) for the removal of emerging contaminants from aquatic environments, *Coord. Chem. Rev.*, 380 (2019) 330–352.
- [35] E. Haque, J.W. Jun, S.H. Jhung, Adsorptive removal of methyl orange and methylene blue from aqueous solution with a metal-organic framework material, iron terephthalate (MOF-235), *J. Hazard. Mater.*, 185 (2011) 507–511.
- [36] A. Mohammadi, A. Alinejad, B. Kamarehie, S. Javan, A. Ghaderpoury, M. Ahmadpour, M. Ghaderpoori, Metal-organic framework UiO-66 for adsorption of methylene blue dye from aqueous solutions, *Int. J. Environ. Sci. Technol.*, 14 (2017) 1959–1968.
- [37] E. García, R. Medina, M. Lozano, I. Hernández Pérez, M. Valero, A. Franco, Adsorption of azo-dye orange II from aqueous solutions using a metal-organic framework material: iron-benzenetricarboxylate, *Materials*, 7 (2014) 8037–8057.
- [38] R.S. Salama, S.A. El-Hakama, S.E. Samraa, S.M. El-Dafrawya, A.I. Ahmeda, Adsorption, Equilibrium and kinetic studies on the removal of methyl orange dye from aqueous solution by using of copper metal-organic framework (Cu-BDC), *Int. J. Mod. Chem.*, 10 (2018) 195–207.
- [39] Z. Saedi, M. Roushani, Influence of amine group on the adsorptive removal of basic dyes from water using two nanoporous isorecticular Zn (II)-based metal-organic frameworks, *Nanochem. Res.*, 3 (2018) 99–108.
- [40] E. Haque, V. Lo, A.I. Minett, A.T. Harris, T.L. Church, Dichotomous adsorption behavior of dyes on an amino-functionalized metal-organic framework, amino-MIL-101 (Al), *J. Mater. Chem. A*, 2 (2014) 193–203.
- [41] C.C. Wang, X.D. Du, J. Li, X.X. Guo, P. Wang, J. Zhang, Photocatalytic Cr(VI) reduction in metal-organic frameworks: a mini-review, *Appl. Catal., B*, 193 (2016) 198–216.
- [42] M.M. Mostafavi, F. Movahedi, Fe₃O₄/MIL-101 (Fe) nanocomposite as an efficient and recyclable catalyst for Strecker reaction, *Appl. Organomet. Chem.*, 32 (2018) e4217.
- [43] Y. Hu, S. Zheng, F. Zhang, Fabrication of MIL-100 (Fe)@SiO₂@Fe₃O₄ core-shell microspheres as a magnetically recyclable solid acidic catalyst for the acetalization of benzaldehyde and glycol, *Front. Chem. Sci. Eng.*, 10 (2016) 534–541.
- [44] R. Karimian, S.J. Davarpanah, MIL-101 (Fe) hexagonal microspindle as a highly efficient, reusable and versatile catalyst for benzo-fused heterocyclic nucleus synthesis, *Appl. Organomet. Chem.*, 32 (2018) e4529.
- [45] H. Lv, H. Zhao, T. Cao, L. Qian, Y. Wang, G. Zhao, Efficient degradation of high concentration azo-dye wastewater by heterogeneous Fenton process with iron-based metal-organic framework, *J. Mol. Catal. A: Chem.*, 400 (2015) 81–89.
- [46] H. Guo, F. Lin, J. Chen, F. Li, W. Weng, Metal-organic framework MIL-125 (Ti) for efficient adsorptive removal of Rhodamine B from aqueous solution, *Appl. Organomet. Chem.*, 29 (2015) 12–19.
- [47] S. Lin, Z. Song, G. Che, A. Ren, P. Li, C. Liu, J. Zhang, Adsorption behavior of metal-organic frameworks for methylene blue from aqueous solution, *Microporous Mesoporous Mater.*, 193 (2014) 27–34.
- [48] M. Abd El-Latif, A.M. Ibrahim, Adsorption, kinetic and equilibrium studies on removal of basic dye from aqueous solutions using hydrolyzed oak sawdust, *Desal. Water Treat.*, 6 (2009) 252–268.
- [49] S.T. Akar, D. Yilmazer, S. Celik, Y.Y. Balk, T. Akar, On the utilization of a lignocellulosic waste as an excellent dye remover: modification, characterization and mechanism analysis, *Chem. Eng. J.*, 229 (2013) 257–266.
- [50] R.E. Khalifa, A.M. Omer, T.M. Tamer, W.M. Salem, M.S.M. Eldin, Removal of methylene blue dye from synthetic aqueous solutions using novel phosphonate cellulose acetate membranes: adsorption kinetic, equilibrium, and thermodynamic studies, *Desal. Water Treat.*, 144 (2019) 272–285.
- [51] X.X. Liang, A. Omer, Z.-h. Hu, Y.g. Wang, D. Yu, X.-k. Ouyang, Efficient adsorption of diclofenac sodium from aqueous solutions using magnetic amine-functionalized chitosan, *Chemosphere*, 217 (2019) 270–278.
- [52] M. Erhayem, F. Al-Tohami, R. Mohamed, K. Ahmida, Isotherm, kinetic and thermodynamic studies for the sorption of mercury (II) onto activated carbon from *Rosmarinus officinalis* leaves, *Am. J. Anal. Chem.*, 6 (2015) 1–10.
- [53] A. Omer, R. Khalifa, Z. Hu, H. Zhang, C. Liu, X.-k. Ouyang, Fabrication of tetraethylenepentamine functionalized alginate

- beads for adsorptive removal of Cr (VI) from aqueous solutions, *Int. J. Biol. Macromol.*, 125 (2019) 1221–1231.
- [54] Y.-S. Ho, G. McKay, Pseudo-second-order model for sorption processes, *Process Biochem.*, 34 (1999) 451–465.
- [55] W.J. Weber, J.C. Morris, Kinetics of adsorption on carbon from solution, *J. Sanit. Eng. Div.*, 89 (1963) 31–60.
- [56] K. Allam, A. El Bouari, B. Belhorma, L. Bih, Removal of methylene blue from water using hydroxyapatite submitted to microwave irradiation, *J. Water Resour. Prot.*, 8 (2016) 358–371.
- [57] R. Tang, C. Dai, C. Li, W. Liu, S. Gao, C. Wang, Removal of methylene blue from aqueous solution using agricultural residue walnut shell: equilibrium, kinetic, and thermodynamic studies, *J. Chem.*, (2017) 8404965.
- [58] E. Ekrami, F. Dadashian, M. Arami, Adsorption of methylene blue by waste cotton activated carbon: equilibrium, kinetics, and thermodynamic studies, *Desal. Water Treat.*, 57 (2016) 7098–7108.
- [59] K. Varaprasad, T. Jayaramudu, E.R. Sadiku, Removal of dye by carboxymethyl cellulose, acrylamide, and graphene oxide via a free radical polymerization process, *Carbohydr. Polym.*, 164 (2017) 186–194.

Supplementary information

Table S1

Specific characteristics of methylene blue (MB) trihydrate dye

Type of dye	Molar mass (g/mol)	Molecular formula	λ_{\max} (nm)
Cationic	373.9	$C_{16}H_{18}N_3SCl_3 \cdot 3H_2O$	664

Table S2

Separation factor (R_L) values for adsorption of MB onto MIL-101(Fe) based on the Langmuir model

C_0 (mg/L)	10	20	30	40	50	100	200
R_L	0.3004	0.1768	0.1252	0.0969	0.0791	0.0412	0.021

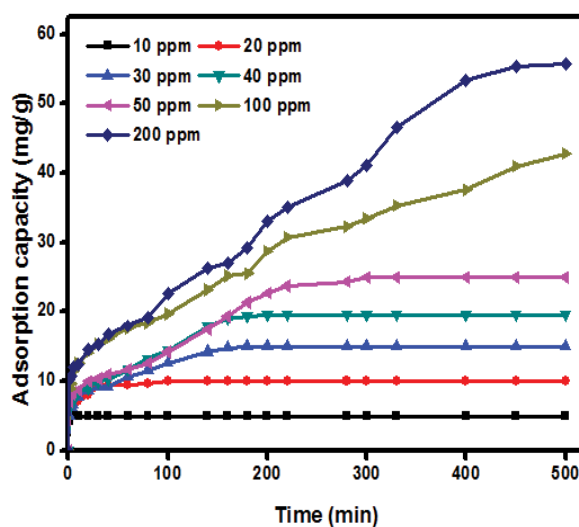


Fig. S1. Adsorption capacity of MB dye onto MIL-101(Fe) with different initial concentrations (10–200 mg/L) using 0.01 g of MIL-101(Fe), (pH 9) and solution temperature (25°C).